ACS APPLIED MATERIALS & INTERFACES

Research Article

www.acsami.org

From Waste to Functional Additive: Toughening Epoxy Resin with Lignin

Wanshuang Liu, Rui Zhou, Hwee Li Sally Goh, Shu Huang, and Xuehong Lu*

School of Materials Science and Engineering, Nanyang Technological University, 50 Nanyang Avenue, Singapore 639798, Singapore

Supporting Information

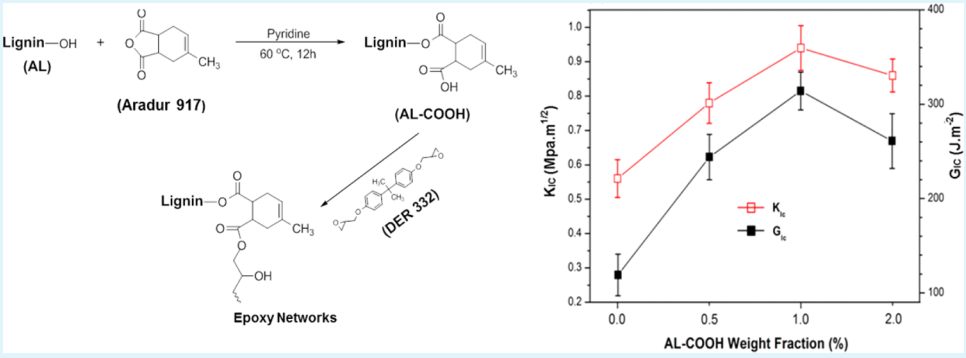

ABSTRACT: A novel approach to toughen epoxy resin with lignin, a common waste material from the pulp and paper industry, is presented in this article. First, carboxylic acid-functionalized alkali lignin (AL-COOH) was prepared and subsequently incorporated into anhydride-cured epoxy networks via a one-pot method. The results of mechanical tests show that covalent incorporation of rigid AL-COOH into epoxy networks can significantly toughen the epoxy matrix without deteriorating its tensile strength and modulus. The addition of 1.0 wt % AL-COOH gives increases of 68 and 164% in the critical stress intensity factor (K_{IC}) and critical strain energy release rate (G_{IC}), respectively, relative to that of neat epoxy. This article opens up the possibility of utilizing low-cost and renewable lignin feedstocks as effective toughening agents for thermoset polymers.

KEYWORDS: *lignin, polymer additive, epoxy resin, toughening*

1. INTRODUCTION

In recent years, there has been increasing interest in the utilization of renewable, biobased feedstocks as advanced materials. Lignin, the second most abundant biopolymer after cellulose, accounts for 20−30% of wood by weight.[1] Lignin has a rigid, hyperbranched macromolecular structure composed of three different types of phenylpropane units and various functional groups, such as hydroxyl, methoxy, ether, aldehyde, and ester groups.[1−3] Although lignin is currently used mainly as fuel, with some simple structural modifications, lignin derivatives have significant potential for value-added products. Therefore, the question how to utilize lignin in various industrial applications has drawn significant attention.

Epoxy resins are one of the most versatile thermosetting polymers with a wide range of applications. The resins are, however, inherently brittle and show poor resistance to crack propagation because of their high degree of chemical cross-linking. Therefore, epoxy toughening has long been an interesting and challenging topic in both academia and industry. So far, the major strategy for toughening epoxy resins is the incorporation of a secondary phase, such as rubber,[4] thermoplastic,[5] clay,[6] CNT,[7] or graphene,[8] into the epoxy matrices, and the phase-separated morphology can induce toughening with various mechanisms. An alternative approach is toughening epoxy resins through lowering the cross-link density of the epoxy networks.[9] The key issue for both approaches is to toughen an epoxy resin without trade-offs in its modulus, mechanical strength, and thermal properties.

In principle, covalent incorporation of stiff macromolecular segments into epoxy networks may improve the toughness of the epoxy matrices by reducing cross-linking density while minimizing the deterioration of the glass-transition temperature and mechanical strength.[10] Lignin is an attractive candidate for such macromolecular toughening agents. In fact, lignin has earlier been suggested to act as a toughener for thermosetting polymers.[11] Thielemans reported that predissolving butyrated lignin as a nonreactive additive could impressively toughen acrylated epoxidized soybean oil−styrene thermosets, with maximum enhancements of 86 and 180% in the critical stress intensity factor (K_{IC}) and critical strain energy release rate (G_{IC}), respectively.[11,12] However, to the best of our knowledge, so far there is no report on toughening effects of lignin for other common thermosetting polymers, including epoxy resins. Several groups have reported the synthesis of lignin-based

Received: January 29, 2014
Accepted: March 24, 2014
Published: March 24, 2014

   dx.doi.org/10.1021/am500642n | ACS Appl. Mater. Interfaces 2014, 6, 5810−5817

epoxy or copolymerization of modified lignin with epoxy, although those studies centered on curing kinetics and thermal properties rather than mechanical properties.[13−15] The hypothesis that lignin could be utilized as macromolecular toughening agents for epoxy resins remains unverified.

The motivation for this work was to investigate whether covalent incorporation of rigid lignin macromolecules into an epoxy network can effectively toughen the epoxy resin as well as to determine if there is a trade-off between toughness and other important properties such as stiffness, strength, and thermal properties. Commercially available lignin, whether from hard or soft wood, is immiscible with most polymers because unmodified lignin tends to aggregate as a result of intermolecular hydrogen bonds, van der Waals interactions between polymer chains, and $\pi-\pi$ stacking of aromatic groups.[16,17] Accordingly, chemical modification of lignin is a necessary process to improve the solubility of lignin in polymers and to introduce reactive sites.[18] In this work, a carboxylic acid-functionalized alkali lignin was prepared through the esterification of hydroxyl groups on the lignin with anhydride, and the modified lignin was subsequently introduced into anhydride-cured epoxy networks via a one-pot method. Herein, we report the significant toughening as well as simultaneous reinforcing effects of the functionalized lignin on the epoxy resin. The underlying mechanism for the toughening effect is also elucidated on the basis of morphological and thermomechanical studies.

2. EXPERIMENTAL SECTION

2.1. Materials. Alkali lignin (AL) was purchased from TCI America (USA, TCI product no. L0082, softwood lignin) and was used after washing with an aqueous 2 M hydrogen chloride (HCl) solution to remove water-soluble impurities and ash. The acid-washing procedure was repeated five times followed by a final wash with distilled water and freeze-drying for 48 h. According to the results of elemental analysis, the contents of elemental hydrogen, nitrogen, and sulfur in AL are 4.93, 0.11, and 1.67 wt %, respectively. Epoxy (DER 332) with an epoxy equivalent weight (the weight of resin containing 1 equiv of epoxy functional group) of 171−175 g per equivalent was supplied by Dow Chemicals (USA). Anhydride hardener (Aradur 917) was supplied by Huntsman Advanced Materials (USA). Zinc acetylacetonate was used as catalyst for the curing reaction and was supplied by Sigma-Aldrich Chemicals Inc. (USA). All other reagents were purchased from Sigma-Aldrich Chemicals Inc. (USA) and were used without further purification. The chemical structures of DER 332 and Aradur 917 are given in Scheme 1.

Scheme 1. Synthesis Routes for the Modified Lignin and Epoxy−Lignin Resins

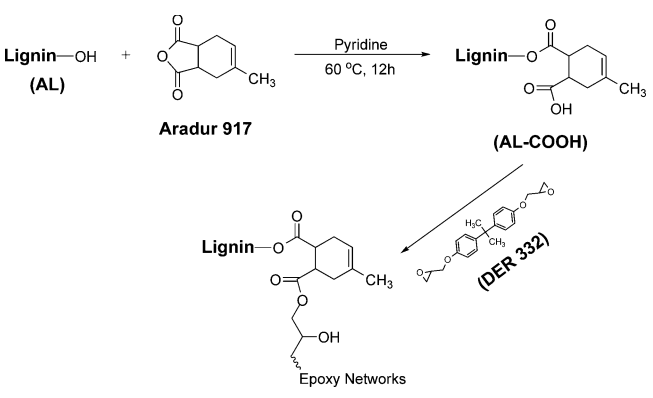

2.2. Hydroxyl Determination of AL. Unmodified AL was acetylated to determine its aliphatic and phenolic hydroxyl content using ^{1}H NMR. Acetylation was performed by dissolving 200 mg of AL in 4 mL of pyridine to form a homogeneous solution. Then, 4 mL of acetic anhydride was added, and the mixture was stirred at 60 °C for 12 h. The reaction solution was then added dropwise to 300 mL of ice water under stirring. The precipitated lignin was collected by filtration through a polycarbonate membrane (0.45 μm), washed with ice−water, and freeze-dried for 48 h.

2.3. Synthesis of Carboxylic Acid-Functionalized Alkali Lignin (AL-COOH). The preparation procedure of AL-COOH was similar to that for the acetylation of AL except that the anhydride used was Aradur 917 instead of acetic anhydride and the final product was further washed with diethyl ether (0.45 μm PTFE membrane was used for this step) to remove excess Aradur 917.

2.4. Preparation of Epoxy−Lignin Resins. A desired amount of AL and 20 mL of pyridine were first added in a one-necked 100 mL flask with magnetic stirring. After AL was fully dissolved in pyridine, 36 g of Aradur 917 was added, and the mixture was heated and kept at 60 °C for 12 h with vigorous stirring in a nitrogen atmosphere. Subsequently, the pyridine was removed by vacuum distillation. Separately, 44.2 g of epoxy monomer and catalyst (zinc acetylacetonate, 1 wt % of the total weight) were mixed homogeneously with a rotary evaporator at 80 °C for half of an hour. Then, all of the components were uniformly mixed together, and the final stoichiometric ratio of epoxy groups to anhydride groups was 100:85. Last, the mixture was poured into a self-made silicone mold and degassed for 4 h at about 0.1 mbar. All samples were cured using the following profile: 80 °C for 2 h, 120 °C for 4 h, and 180 °C for 4 h. Neat epoxy was prepared following the same procedure as mentioned above. Samples for mechanical testing were prepared by curing in the silicone molds with specific dimensions.

2.5. Characterization. Fourier transform infrared (FTIR) spectra were obtained using a PerkinElmer Instruments Spectrum GX FTIR spectrometer at room temperature in the wavenumber range of 600−4000 cm^{-1}. ^{1}H NMR was measured using a Bruker Avance 300 MHz spectrometer equipped with autotunable BBO probe. For quantitative ^{1}H NMR, precisely 10 mg of acetylated lignin was dissolved in 0.5 mL of DMSO-d_6. Pentafluorobenzaldehyde (PFB) (10 μL) was accurately added into a NMR tube using a pipet at 60 °C as an internal standard. Dynamic rheological measurements were performed on a Rheometer MCR 501 from Anton Paar Inc. Elemental analysis was performed using PerkinElmer Instruments CHNS-O analyzer. Differential scanning calorimetry (DSC) was recorded on a TA Instruments DSC Q10 using N_2 as the purge gas at a heating rate of 2 °C min^{-1}. Dynamic mechanical analysis (DMA) was conducted on a TA Instruments DMA Q800 at a heating rate of 3 °C min^{-1} and a frequency of 1 Hz under an air atmosphere. The tests were carried out using the single cantilever mode, and the specimen dimensions were 40 × 13.0 × 2.0 mm^3. Thermal mechanical analysis (TMA) data were measured on a TA Instruments TMA-2940 analyzer. The dimensions of the cuboid-shaped specimen were 8.0 × 8.0 × 4.0 mm^3. The temperature was increased at a rate of 10 °C min^{-1} during the measurements. Linear regressions were conducted to estimate CTE values in different temperature regions. Thermal gravimetric analysis (TGA) was performed on a TA Instruments TGA Q500 under an air atmosphere over a temperature range of 25−800 °C at a heating rate of 10 °C min^{-1}. Tensile tests were performed using an ITW Instron Tester 5567 with a 3 kN load cell at a crosshead speed of 1 mm min^{-1}. Dog-bone-shaped tensile samples were prepared according to the ASTM D638 standard. Each reported value was the average of at least 10 specimens. Fracture toughness of the samples was measured according to the ASTM D5045 standard using a three-point-bend (SEN-3PB) single-edge-notch specimen with geometry of 53 × 12 × 6 mm^3. A sharpened notch was machined at the midpoint of each specimen by a fine band saw. A precrack was then initiated by tapping a fresh razor blade in the notch. The specimens were loaded to failure at a crosshead speed of 1 mm min^{-1} using an Instron Micro Tester 5848 equipped with a 2 kN load cell. Critical stress intensity factor (K_{IC}) and critical strain energy release rate (G_{IC}) were calculated in

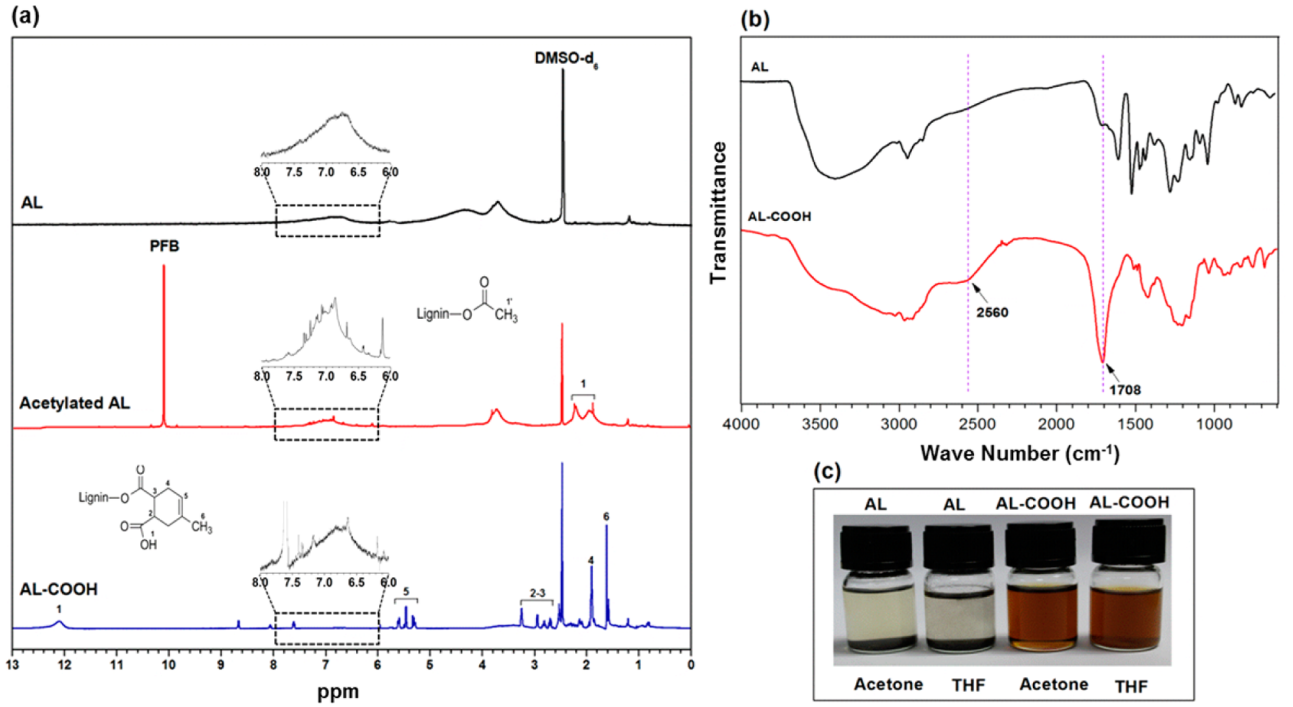

Figure 1. (a) ^{1}H NMR spectra of AL, acetylated AL, and AL-COOH; (b) FTIR spectra of AL and AL-COOH; (c) solubility of AL and AL-COOH in acetone and THF (concentration = 2 mg mL^{-1}).

accordance with the ASTM D5045 standard. Each reported value was the average of at least 10 specimens. The fracture surfaces from fracture toughness tests were investigated by a JEOL FESEM 7600F field-emission scanning electron microscope (FESEM). The samples were coated with gold. Optical microscopy observation was conducted on a Nikon Eclipse LV100. Transmission electron microscopy (TEM) was performed on a JEOL-2010 with an accelerating voltage of 200 kV. The samples were prepared by ultramicrotome with a thickness of 50−70 nm at room temperature in water.

3. RESULTS AND DISCUSSION

3.1. Modification of Lignin. AL is generally produced from wood pulping using the kraft and soda methods, which are based on treatments with sodium sulfate plus sodium hydroxide or sodium hydroxide alone.[19] Among various functional groups on lignin, phenolic and aliphatic hydroxyl groups are the most abundant reactive sites and have been exploited for the functionalization of lignin through reaction with bromoalkane, carboxylic acid, carboxylic acid halide, or anhydride.[11,20] In this work, AL was modified by pyridine-catalyzed esterification with anhydrides, as presented in Scheme 1. First, the total concentration of hydroxyl groups was determined by ^{1}H NMR of acetylated AL. The AL used in this study contains 5.6 mmol g^{-1} of hydroxyl groups based on the calculation from the integrals of proton resonances in acetoxy groups (1.5−2.4 ppm) and PFB (10.1 ppm),[2] as shown in Figure 1a. ^{1}H NMR of AL-COOH and corresponding proton assignments are also shown in Figure 1a, where the resonances at 12.1, 5.3−5.6, and 1.6 ppm are assigned to the protons in −COOH, −CH═CH−, and CH_3−C═C− groups, respectively. The magnified spectra between 6 and 8 ppm in Figure 1a show the proton resonances from aromatic groups of AL and modified AL. The structure of AL-COOH is further confirmed by the FTIR spectra (Figure 1b). Compared with unmodified AL, AL-COOH shows a broad carboxylic band in the region of 2500−3500 cm^{-1} and a significant carbonyl (C═O) signal at 1708 cm^{-1}. Owing to the chemical modification, AL-COOH exhibits improved organic compatibility. In sharp contrast to AL, AL-COOH can be well-dissolved in acetone and THF (Figure 1c).

3.2. Effects of AL-COOH on Rheological Properties and Curing Behaviors. Viscosity is a very important parameter for the processability of an epoxy resin. The rheological behaviors of uncured neat epoxy resin and the epoxy precursors with different AL-COOH loadings are shown in Figure 2. All of the samples behave as non-Newtonian fluids and exhibit shear thinning. As expected, the viscosity (η) increases with the increase of AL-COOH loading. Compared with neat epoxy (shear rate = 1.0 s^{-1}), the viscosity of epoxy−lignin resins increases by about 1.9-, 2.8-, and 11.4-fold when

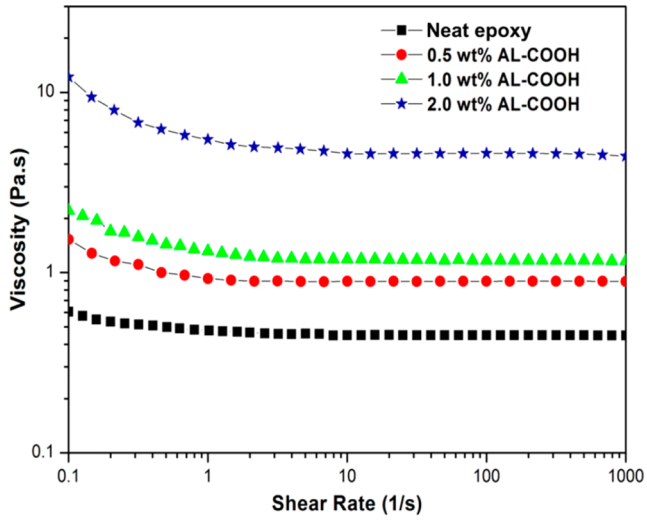

Figure 2. Viscosity versus shear rate of uncured neat epoxy and epoxy−lignin resins with different AL-COOH loadings.

dx.doi.org/10.1021/am500642n | ACS Appl. Mater. Interfaces 2014, 6, 5810−5817

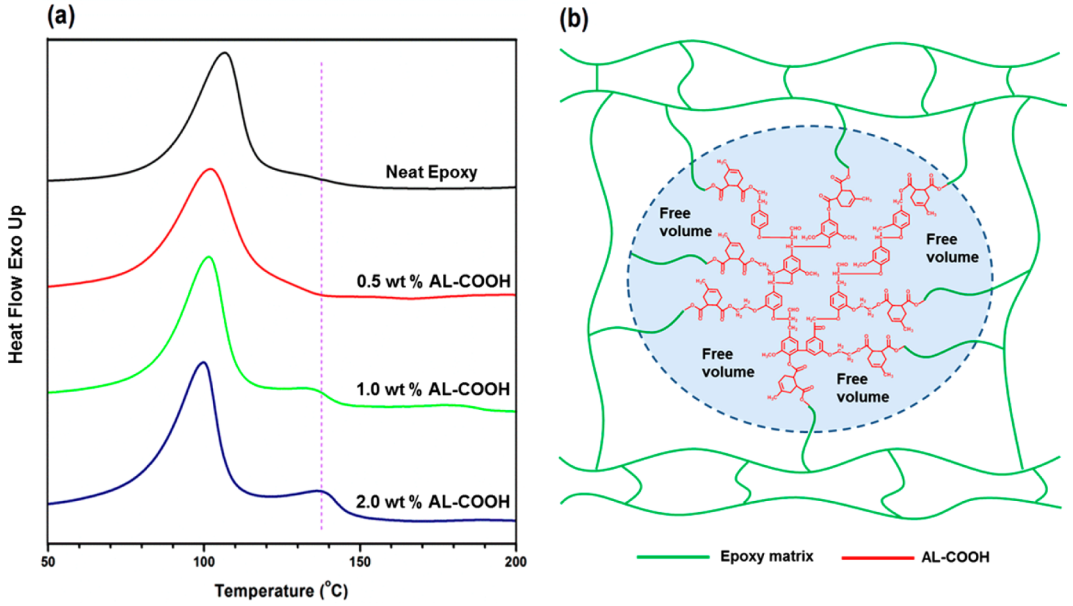

Figure 3. (a) DSC thermograms of neat epoxy and the epoxy−lignin resins with different AL-COOH loadings and (b) schematic illustration of the structure of the epoxy−lignin resins.

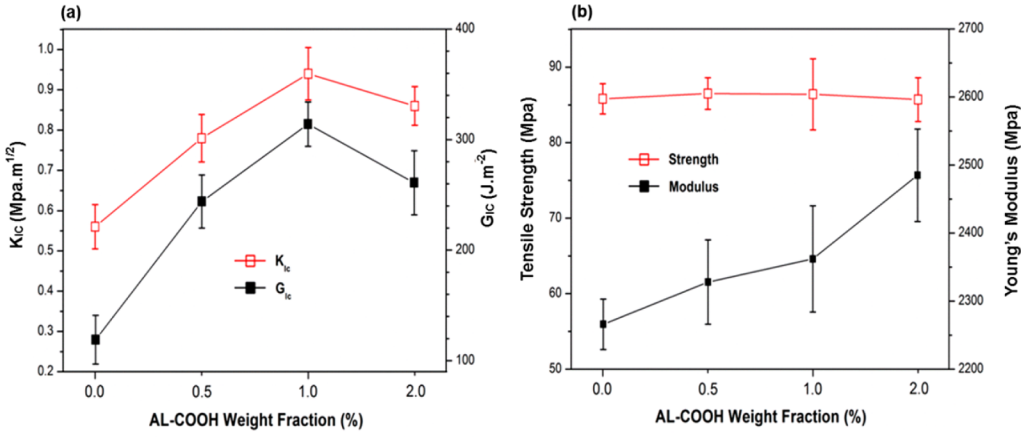

Figure 4. Fracture toughness (a) and tensile properties (b) of neat epoxy and the epoxy−lignin resins with different AL-COOH loadings.

0.5, 1.0, and 2.0 wt % AL-COOH were added, respectively (Table S1 in the Supporting Information).

Because lignin is a rigid and hyperbranched macromolecule, it is essential to investigate the influence of introducing AL-COOH on the curing behaviors of the epoxy−anhydride system. Figure 3a shows the DSC exothermic curves of neat epoxy and epoxy−lignin resins with different AL-COOH loadings, and the data are summarized in Table S1 in the Supporting Information. It was found that AL-COOH has almost no effect the main exothermal peak temperature, implying that the incorporation of AL-COOH does not significantly alter the activation energy of the curing reaction. However, a new exothermal peak appears at around 130−140 °C, and its intensity increases with increasing AL-COOH loading. The new exothermal peak is very likely to arise from the reaction between carboxyl groups of AL-COOH and epoxy groups of DER 332 because it has been reported that this reaction can occur even without catalyst in the temperature range of 100−170 °C.[21]

To confirm further that AL-COOH molecules participated in the curing reaction, the reaction between DER 332 and AL-COOH was studied by DSC and FTIR. A mixture containing 25 wt % AL-COOH, 75 wt % DER 332, and a catalytic amount of zinc acetylacetonate was used for the tests. The details of the sample preparation and test conditions are described in the Supporting Information. Figure S1 in the Supporting Information shows the DSC exothermic curve for the mixture of AL-COOH and DER 332. As can be seen, one exothermal peak with peak exothermal temperature at ∼132 °C was observed, which is consistent with the new exothermal peak found in Figure 3a and the reported reaction temperature between carboxyl groups and epoxy groups.[21] Another exothermal peak starts to appear at about 200 °C, which may be attributed to the etherification between hydroxyl groups and excess epoxy groups.[21] Figure S2 in the Supporting Information shows the FTIR spectra of DER 332, AL-COOH, and their mixture after heating at 180 °C for 4 h. The spectrum of the mixture after heating shows that the characteristic peaks of carboxyl groups (broad band in the region of 2500−3500 cm^{-1} and carbonyl signal at 1708 cm^{-1}) almost disappear and that a sole carbonyl signal (1730 cm^{-1}) from ester groups remains. According to these results, it is concluded that AL-COOH was

dx.doi.org/10.1021/am500642n | ACS Appl. Mater. Interfaces 2014, 6, 5810−5817

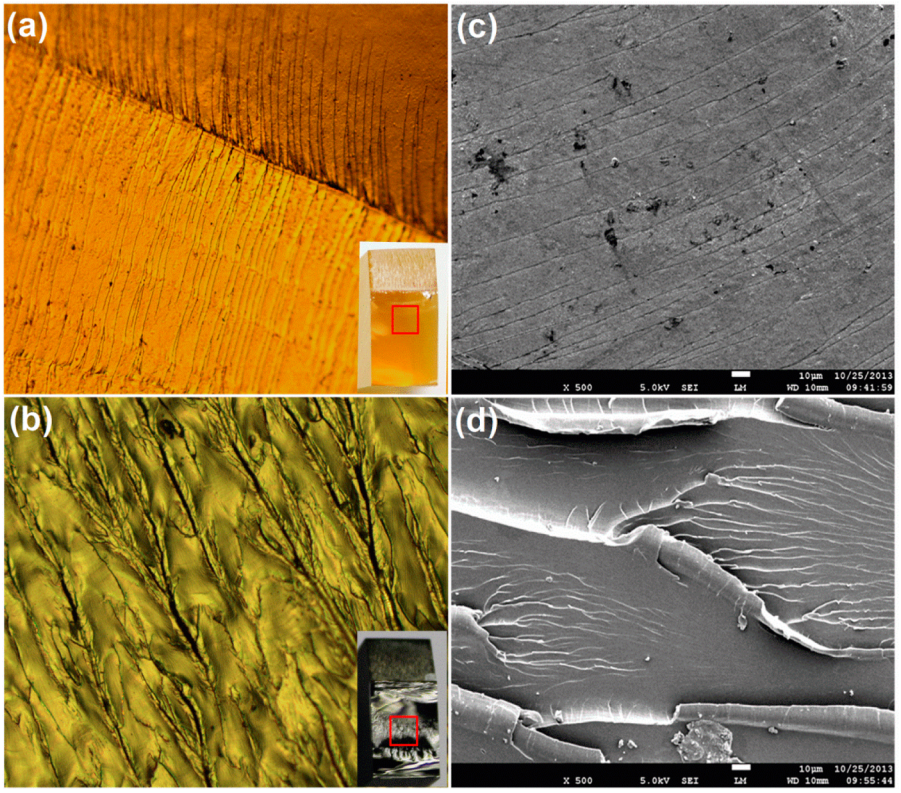

Figure 5. Optical microscopy images (×200) showing the fracture surfaces of neat epoxy (a) and the epoxy−lignin resin with 1.0 wt % AL-COOH (b); the insets show the observed regions. SEM images (×500) showing the fracture surfaces of neat epoxy (c) and the same epoxy−lignin resin (d).

indeed covalently incorporated into the epoxy network, as illustrated in Scheme 1 and Figure 3b.

In addition, the total enthalpy values (ΔH) for the entire curing temperature range were observed to decrease with increasing AL-COOH loading (Table S1 in the Supporting Information), indicating that the incorporation of bulky lignin molecules decreases the degree of cross-linking. Quantitative changes in the cross-linking density when AL-COOH was incorporated will be further discussed later on the basis of the DMA results. The dispersion state of AL-COOH in the epoxy matrix during the curing process was also investigated. The mixture remains transparent throughout the curing process, and TEM observation showed that no particles or cavities were observed in the epoxy−lignin resin, indicating that no phase separation occurs (Figure S3 in the Supporting Information).

3.3. Mechanical Properties. Fracture toughness and tensile tests were performed to evaluate the reinforcing and toughening effects of the incorporated AL-COOH. Figure 4a shows the fracture toughness of the epoxy resins with different contents of AL-COOH. Both the critical stress intensity factor (K_{IC}) and the critical strain energy release rate (G_{IC}) were distinctly improved with the incorporation of AL-COOH. Among all samples, the one with 1.0 wt % AL-COOH showed the best toughening effect with a 68% increase in K_{IC} and 164% increase in G_{IC} with respect to those of neat epoxy. However, tensile test results show that Young's modulus also increases with AL-COOH loading, whereas the addition of AL-COOH had almost no influence on the tensile strength (Figure 4b). The sample with 2.0 wt % AL-COOH showed the maximum average modulus of 2485 ± 68 MPa, an improvement of about 10% compared with that of neat epoxy. Therefore, unlike toughening epoxy with rubber particles,[4] incorporation of AL-COOH into epoxy networks can toughen the epoxy resins without sacrificing the stiffness of the resultant materials. It should be noted that the elongation at break decreases with increasing AL-COOH loading (Table S2 in the Supporting Information), indicating that in the tensile process the rigid AL-COOH cannot accommodate the same strain as the epoxy matrix.

The morphology of the fracture surface of neat epoxy and the epoxy−lignin resins was investigated by optical microscopy and SEM. Figure 5 shows the representative microscopic images of the fracture surfaces of neat epoxy and an epoxy−lignin resin near the crack initiation site. The fracture surface of neat epoxy (Figure 5a,c) is very smooth except for some river-like lines, indicating a brittle failure mode without any ductility. In contrast, the fracture surface of the epoxy−lignin resin with 1.0 wt % AL-COOH is rougher, and a large plastic deformation was observed (Figure 5b,d). Furthermore, large-area crazing was also observed. Plastic deformation and crazing are significant energy-absorbing processes; thus, they result in an increase in the amount of energy needed for crack propagation and for the formation of new surfaces. This difference in fracture behaviors confirms the toughening effect induced by the incorporation of AL-COOH. More micrographs of fracture surfaces are provided in Figures S4 and S5 in the Supporting Information.

3.4. Dynamic Mechanical Properties. To gain further insight into the toughening and reinforcing effects observed, dynamic mechanical behaviors of neat epoxy and the epoxy−lignin resins were measured. The curves of the storage modulus (E'), loss modulus (E''), and tan δ versus temperature are given in Figure 6, and the data are summarized in Table 1. Compared with neat epoxy, epoxy−lignin resin shows continuous improvement in E' in the glassy region with increasing AL-

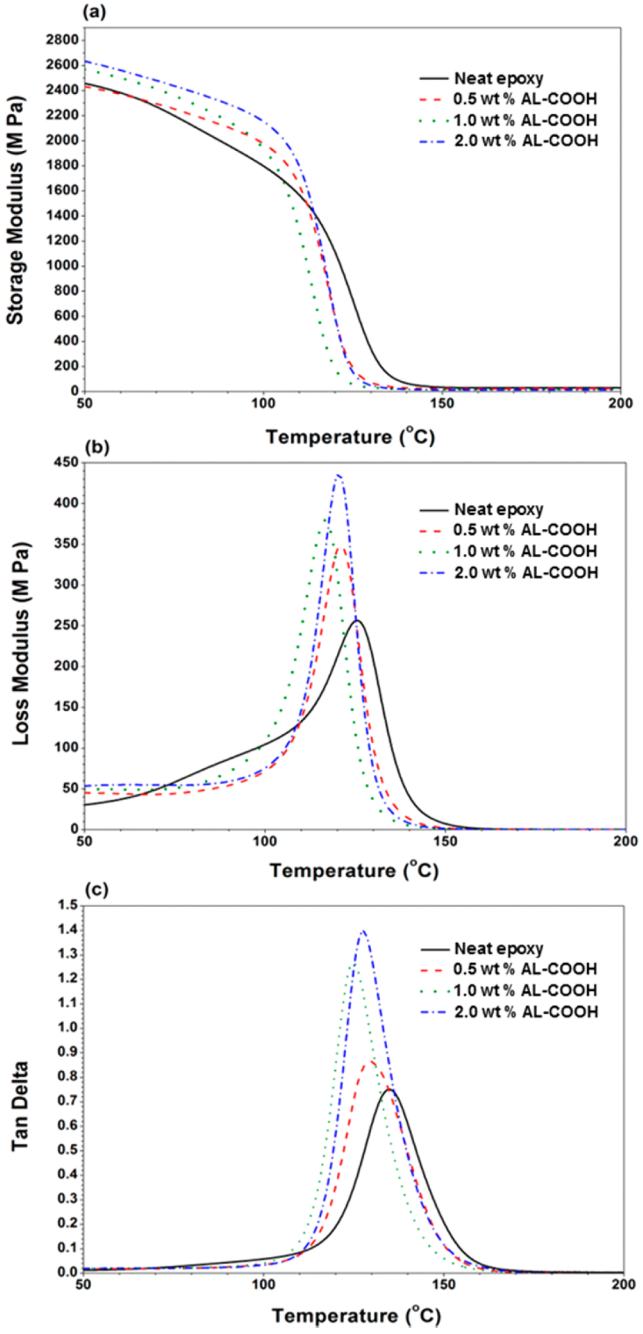

Figure 6. Storage modulus (a), loss modulus (b), and tan δ (c) versus temperature for the neat epoxy and epoxy–lignin resins with different AL-COOH loadings.

COOH loading with the exception of the sample with 0.5 wt % AL-COOH, which shows a slightly decreased E'. The increase in E' may be due to the segmental confinement imposed by the uniformly dispersed rigid AL-COOH in the epoxy matrix.

According to the theory of rubber elasticity, the cross-linking density (ρ) of a cured epoxy network is proportional to its storage modulus in the rubbery region, and the cross-linking density can be calculated using the equation

$$\rho = E'/3RT \quad (1)$$

where E' is the storage modulus at T_g + 30 °C, R is the gas constant, and T is the absolute temperature at T_g + 30 °C.[22] Compared with neat epoxy, the cross-link densities of the epoxy–lignin samples monotonously decrease with increasing AL-COOH loading (Table 1). This is presumably due to the relative low carboxylic content of the AL-COOH molecules, which was determined from the quantitative ^{1}H NMR analysis. Additionally, the steric hindrance of bulk lignin also restrains the curing reaction, which was confirmed by the DSC results.

The loss modulus represents the energy dissipation because of the internal friction related to the motion of the polymer chain. As can be clearly seen in Table 1, the maximum of loss modulus continues to increase from 256 to 436 MPa as the AL-COOH loading increases up to 2.0 wt %. This indicates that the mobility of the polymer chains is improved in the glass-transition process when AL-COOH is incorporated, which is consistent with the decreased cross-link densities of the epoxy–lignin resins. Tan δ is defined as the ratio of the loss modulus to the storage modulus, and the peak of the tan δ versus temperature curve is taken as glass-transition temperature (T_g). As shown in Figure 6c, all of the samples show one narrow and smooth α-relaxation peak that corresponds to the glass transition. As expected, T_g values of the epoxy–lignin resins (125–130 °C) are slightly lower than that of neat epoxy (134 °C) because of their decreased cross-linking densities. Another evidence for the variation of T_g is from the DSC results. Figure S6 in the Supporting Information shows the DSC curves of the cured resins. It can be seen that the T_g values of the epoxy–lignin resins (110–114 °C) are slight lower than that of neat epoxy (116 °C), which is consistent with the results of DMA.

3.5. Thermal Expansion. The values of the coefficient of thermal expansion (CTE) measured in the glassy region (α_g) and the rubber region (α_r) as well as their difference ($\Delta\alpha = \alpha_r - \alpha_g$) are listed in Table 2. The epoxy–lignin resins showed higher CTE values compared with neat epoxy, especially in the rubbery region because of their lower cross-link density.[23] Besides the cross-link density, CTE was also affected by the variation in the free volume caused by the incorporation of rigid AL-COOH. According to classic free-volume theory,[24,25] the free-volume fraction (V_g) at T_g can be calculated as

Table 1. DMA Results of Neat Epoxy and the Epoxy–Lignin Resins

composition	storage modulus (MPa)		maximum loss modulus (MPa)	T_g (°C)	ρ (10^{-3} mol cm^{-3})
	glassy region[a]	rubbery region[b]			
neat epoxy	2456	30	256	134	2.75
0.5 wt % AL-COOH	2422	24	347	130	2.22
1.0 wt % AL-COOH	2557	19	380	125	1.79
2.0 wt % AL-COOH	2633	13	436	127	1.21

[a]At 50 °C. [b]At T_g + 30 °C.

dx.doi.org/10.1021/am500642n | ACS Appl. Mater. Interfaces 2014, 6, 5810–5817

Table 2. TMA Results of Neat Epoxy and the Epoxy−Lignin Resins

composition	α_g (10^{-6} K^{-1})	α_r (10^{-6} K^{-1})	$\Delta\alpha = \alpha_g - \alpha_r$ (10^{-6} K^{-1})
neat epoxy	65.0	176.7	111.7
0.5 wt % AL-COOH	70.3	191.5	121.2
1.0 wt % AL-COOH	71.2	198.3	127.1
2.0 wt % AL-COOH	70.4	206.8	136.4

$$V_g = \left(\frac{\Delta\alpha B \frac{C_2}{C_1}}{2.303} \right)^{1/2} \quad (2)$$

where B is a constant generally considered to be close to unity and C_1 and C_2 are the WLF constants. In the equation, V_g is proportional to $\Delta\alpha$. Therefore, the increased $\Delta\alpha$ for the epoxy−lignin resins (Table 2) may indicate the existence of more free volume when rigid and hyperbranched AL-COOH is incorporated into the epoxy networks. This assertion is consistent with previous reports that utilized positron annihilation lifetime spectroscopy measurements and confirmed that introducing a hyperbranched polymer into epoxy networks can increase the free volume.[26,27]

3.6. Toughening Mechanism. It is known that phase-separated morphology is normally required to initiate various toughening mechanisms for rubber- and thermoplastic-toughened epoxy resins.[4,5] However, the epoxy−lignin system showed no phase separation according to TEM studies. In conjunction with the results from DSC and DMA, it was confirmed that AL-COOH is integrated into the epoxy network at the molecular level. Therefore, unlike those from dispersed particles, the toughening effect from the incorporated AL-COOH originates from the variation of epoxy network architecture. The decrease in the cross-linking density is likely to be the major reason for the improvement in fracture toughness.[9] In addition, the increased free volume may also contribute to the improved fracture toughness. Overall, the significant toughness enhancement accompanied by the moderate improvement in stiffness for the epoxy−lignin resin should arise from a balance of the segmental confinement effects, decreased cross-linking density, and increased free volume.

3.7. Thermogravimetric Analysis. Thermal stability of AL-COOH, neat epoxy, and epoxy−lignin resins was evaluated by TGA in an air atmosphere. The TGA curves are shown in Figure 7, and the data are summarized in Table S3 in the Supporting Information. There are two degradation stages for both neat epoxy and epoxy−lignin resins, which are related to the degradation of aliphatic (first stage) and aromatic (second stage) components of the epoxy matrix, respectively.[28] Compared with neat epoxy (303 °C), the composites show lower onset degradation temperatures (262−273 °C). This is due to the lower thermal stability of lignin. It has been reported that thermal degradation of lignin occurs slowly under a wide temperature range from ambient to 800 °C because of the complex structure of lignin.[29,30] In addition, the char yield of the epoxy−lignin resins increases with an increase in AL-COOH loading because of the high content of aromatic components in lignin.

4. CONCLUSIONS

AL-COOH was prepared and incorporated into an anhydride-cured epoxy via a one-pot method. The fracture toughness of the epoxy−lignin resin is drastically improved compared with neat epoxy. In particular, the sample with 1.0 wt % AL-COOH showed large increases of 68 and 164% in K_{IC} and G_{IC}, respectively, relative to that of neat epoxy. It is noteworthy that the tensile strength of the epoxy−lignin resin is almost the same as that of neat epoxy, whereas the Young's modulus of the epoxy−lignin resin increases moderately with increasing AL-COOH loading. The toughning effect of the functionalized lignin was further confirmed by microscopic observation of fracture surfaces. According to the results of DMA, TMA, and TEM observation, the toughening effects are considered to arise mainly from the decreased cross-linking density and the increased free volume of the epoxy−lignin resin. We believe that the effectively toughened epoxy resins with low-cost, biorenewable lignin have considerable potantial for use as durable coating materials or matrix materials for high-performance composites.

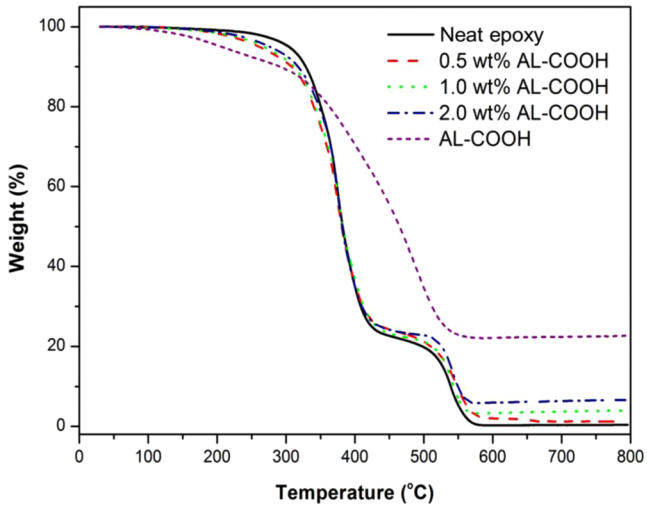

Figure 7. TGA curves of AL-COOH, neat epoxy, and epoxy−lignin resins with different AL-COOH loadings.

■ ASSOCIATED CONTENT

Supporting Information

Data of DSC and rheological properties of neat epoxy and the epoxy−lignin resins; DSC thermogram for mixture of DER 332, AL-COOH, and zinc acetylacetonate; FTIR spectra of DER 332, AL-COOH, and a mixture of DER 332, AL-COOH, and zinc acetylacetonate after heating; dispersion of AL-COOH in the epoxy matrix; mechanical properties; optical microscopy and SEM observation of fracture surface; and TGA data. This material is available free of charge via the Internet at http://pubs.acs.org.

■ AUTHOR INFORMATION

Corresponding Author

*E-mail: asxhlu@ntu.edu.sg; Tel: +65 9847 6690.

Notes

The authors declare no competing financial interest.

■ ACKNOWLEDGMENTS

This work was supported by the Science and Engineering Research Council of the Agency for Science, Technology and Research (A*STAR), Singapore, under grant no. 11 2300 4027.

■ REFERENCES

(1) Calvo-Flores, F. G.; Dobado, J. A. Lignin as Renewable Raw Material. *ChemSusChem* **2010**, *3*, 1227−1235.
(2) Chung, H.; Washburn, N. R. Improved Lignin Polyurethane Properties with Lewis Acid Treatment. *ACS Appl. Mater. Interfaces* **2012**, *4*, 2840−2846.
(3) Saito, T.; Brown, R. H.; Hunt, M. A.; Pickel, D. L.; Pickel, J. M.; Messman, J. M.; Baker, F. S.; Keller, M.; Naskar, A. K. Turning Renewable Resources into Value-Added Polymer: Development of Lignin-Based Thermoplastic. *Green Chem.* **2012**, *14*, 3295−3303.
(4) Bagheri, R.; Marouf, B. T.; Pearson, R. A. Rubber-Toughened Epoxies: A Critical Review. *Polym. Rev.* **2009**, *49*, 201−225.
(5) Hodgkin, J. H.; Simon, G. P.; Varley, R. J. Thermoplastic Toughening of Epoxy Resins: A Critical Review. *Polym. Adv. Technol.* **1998**, *9*, 3−10.
(6) Wang, K.; Chen, L.; Wu, J.; Toh, M. L.; He, C.; Yee, A. F. Epoxy Nanocomposites with Highly Exfoliated Clay: Mechanical Properties and Fracture Mechanisms. *Macromolecules* **2005**, *38*, 788−800.
(7) Gojny, F. H.; Wichmann, M. H. G.; Fiedler, B.; Schulte, K. Influence of Different Carbon Nanotubes on the Mechanical Properties of Epoxy Matrix Composites − A Comparative Study. *Compos. Sci. Technol.* **2005**, *65*, 2300−2313.
(8) Rafiee, M. A.; Rafiee, J.; Wang, Z.; Song, H.; Yu, Z.; Koratkar, N. Enhanced Mechanical Properties of Nanocomposites at Low Graphene Content. *ACS Nano* **2009**, *3*, 3884−3890.
(9) Sherman, C. L.; Zeigler, R. C.; Verghese, N. E.; Marks, M. J. Structure-Property Relationships of Controlled Epoxy Networks with Quantified Levels of Excess Epoxy Etherification. *Polymer* **2008**, *49*, 1164−1172.
(10) Pham, H. Q.; Marks, M. J. Epoxy Resins. *Ullmann's Encyclopedia of Industrial Chemistry*; Wiley-VCH: Weinheim, Germany, 2000; pp 219−220.
(11) Wool, R. P., Sun, X. S. *Bio-Based Polymers and Composites*; Elsevier: Amsterdam, 2005; pp 551−598.
(12) Thielemans, W. Lignin and Carbon Nanotube Utilization in Bio-Based Composites. Ph.D. Thesis, University of Delaware, Newark, DE, 2004.
(13) Sun, G.; Sun, H.; Liu, Y.; Zhao, B.; Zhu, N.; Hu, K. Comparative Study on the Curing Kinetics and Mechanism of a Lignin-Based-Epoxy/Anhydride Resin System. *Polymer* **2007**, *48*, 330−337.
(14) Mansouri, N. E.; Yuan, Q.; Huang, F. Synthesis and Characterization of Kraft Ligninbased Epoxy Resins. *BioResources* **2011**, *6*, 2492−2503.
(15) Raquez, J. M.; Deleglise, M.; Lacrampe, M. F.; Krawczak, P. Thermosetting (Bio)Materials Derived from Renewable Resources: A Critical Review. *Prog. Polym. Sci.* **2010**, *35*, 487−509.
(16) Chung, Y.; Olsson, J. V.; Li, R. J.; Frank, C. W.; Waymouth, R. M.; Billington, S. L.; Sattely, E. S. A Renewable Lignin−Lactide Copolymer and Application in Biobased Composites. *ACS Sustainable Chem. Eng.* **2013**, *1*, 1231−1238.
(17) Deng, Y.; Feng, X.; Zhou, M.; Qian, Y.; Yu, H.; Qiu, X. Investigation of Aggregation and Assembly of Alkali Lignin Using Iodine as a Probe. *Biomacromolecules* **2011**, *12*, 1116−1125.
(18) Thielemans, W.; Wool, R. P. Lignin Esters for Use in Unsaturated Thermosets: Lignin Modification and Solubility Modeling. *Biomacromolecules* **2005**, *6*, 1895−1905.
(19) Meister, J. J. Modification of Lignin. *J. Macromol. Sci., Polym. Rev.* **2002**, *C42*, 235−289.
(20) Sen, S.; Sadeghifar, H.; Argyropoulos, D. S. Kraft Lignin Chain Extension Chemistry via Propargylation, Oxidative Coupling, and Claisen Rearrangement. *Biomacromolecules* **2013**, *14*, 3399−3408.
(21) Han, S. O.; Drzal, L. T. Curing Characteristics of Carboxyl Functionalized Glucose Resin and Epoxy Resin. *Eur. Polym. J.* **2003**, *39*, 1377−1384.
(22) Kaji, M.; Nakahara, K.; Endo, T. Synthesis of a Bifunctional Epoxy Monomer Containing Biphenyl Moiety and Properties of Its Cured Polymer with Phenol Novolac. *J. Appl. Polym. Sci.* **1999**, *74*, 690−698.
(23) Komarov, P. V.; Chui, Y.; Chen, S.; Khalatur, P. G.; Reineker, P. Highly Cross-Linked Epoxy Resins: An Atomistic Molecular Dynamics Simulation Combined with a Mapping/ Reverse Mapping Procedure. *Macromolecules* **2007**, *40*, 8104−8113.
(24) Montazeri, A.; Pourshamsian, K.; Riazian, M. Viscoelastic Properties and Determination of Free Volume Fraction of Multi-Walled Carbon Nanotube/Epoxy Composite Using Dynamic Mechanical Thermal Analysis. *Mater. Des.* **2012**, *36*, 408−414.
(25) Williams, M. L.; Landel, R. F.; Ferry, J. D. The Temperature Dependence of Ralaxation Mechanisms in Amorphous Polymers and Other Glass-Forming Liquids. *J. Am. Chem. Soc.* **1955**, *77*, 3701−3707.
(26) Luo, L.; Qiu, T.; Meng, Y.; Guo, L.; Yang, J.; Li, Z.; Cao, X.; Li, X. A Novel Fluoro-Terminated Hyperbranched Poly(phenylene oxide) (FHPPO): Synthesis, Characterization, and Application in Low-*k* Epoxy Materials. *RSC Adv.* **2013**, *3*, 14509−14520.
(27) Ratna, D.; Simon, G. P. Epoxy and Hyperbranched Polymer Blends: Morphology and Free Volume. *J. Appl. Polym. Sci.* **2010**, *117*, 557−564.
(28) Wang, D. H.; Sihn, S.; Roy, A. K.; Baek, J. B.; Tan, L. S. Nanocomposites Based on Vapor-Grown Carbon Nanofibers and an Epoxy: Functionalization, Preparation and Characterization. *Eur. Polym. J.* **2010**, *46*, 1404−1416.
(29) Yang, H.; Yan, R.; Chen, H.; Lee, D. H.; Zheng, C. Characteristics of Hemicellulose, Cellulose and Lignin Pyrolysis. *Fuel* **2007**, *86*, 1781−1788.
(30) Kim, J. Y.; Oh, S.; Hwang, H.; Kim, U. J.; Choi, J. W. Structural Features and Thermal Degradation Properties of Various Lignin Macromolecules Obtained from Poplar Wood (*Populus albaglandulosa*). *Polym. Degrad. Stab.* **2013**, *98*, 1671−1678.